

SCIENTIFIC REPORTS



OPEN

Horizontally-acquired genetic elements in the mitochondrial genome of a centrohelid *Marophrys* sp. SRT127

Yuki Nishimura^{1,4}, Takashi Shiratori^{1,5}, Ken-ichiro Ishida¹, Tetsuo Hashimoto^{1,2}, Moriya Ohkuma³ & Yuji Inagaki^{1,2}

Mitochondrial genomes exhibit diverse features among eukaryotes in the aspect of gene content, genome structure, and the mobile genetic elements such as introns and plasmids. Although the number of published mitochondrial genomes is increasing at tremendous speed, those of several lineages remain unexplored. Here, we sequenced the complete mitochondrial genome of a unicellular heterotrophic eukaryote, *Marophrys* sp. SRT127 belonging to the Centroheliozoa, as the first report on this lineage. The circular-mapped mitochondrial genome, which is 113,062 bp in length, encodes 69 genes typically found in mitochondrial genomes. In addition, the *Marophrys* mitochondrial genome contains 19 group I introns. Of these, 11 introns have genes for homing endonuclease (HE) and phylogenetic analyses of HEs have shown that at least five *Marophrys* HEs are related to those in green algal plastid genomes, suggesting intron transfer between the *Marophrys* mitochondrion and green algal plastids. We also discovered a putative mitochondrial plasmid in linear form. Two genes encoded in the circular-mapped mitochondrial genome were found to share significant similarities to those in the linear plasmid, suggesting that the plasmid was integrated into the mitochondrial genome. These findings expand our knowledge on the diversity and evolution of the mobile genetic elements in mitochondrial genomes.

Mitochondria have emerged by the endosymbiosis between the last common ancestor of eukaryotes and an α -proteobacterium. All extant eukaryotes have mitochondria or mitochondrial remnant organelles, with only one exception of *Monocercomonoides* sp. PA203¹ (now classified as *Monocercomonoides exilis*²). Although most of the genes in the α -proteobacterium that gave rise to the ancestral mitochondrion have been lost or transferred to the host nucleus during organogenesis, typical mitochondria, which can carry out aerobic respiration, still retain their genomes³ (mitochondrial genomes, mtDNAs). The gene repertoires in mtDNAs have differently reduced in individual lineages in eukaryotes from the ancestral mtDNA that encoded at least about 100 genes for oxidative phosphorylation, translation, transcription, protein transport, protein maturation and RNA processing as found in mtDNA of jakobids^{4,5}. In contrast, apicomplexan parasites and their relatives have only three to five genes in their mtDNAs⁶. mtDNAs also vary with regard to genome architecture, from a simple monocircular molecule (e.g., human mtDNA) to a complex network comprising thousands of chromosomes (e.g., mtDNAs in kinetoplasts). Monoliner mtDNAs were reported from separate branches of eukaryotes as well as mtDNAs consisting of multiple linear chromosomes^{7–11}. Likewise, the size range of mtDNA is broad among eukaryotes. Apicomplexan parasites are known to have the smallest mtDNAs, approximately 6 Kb in size⁸. On the other hand, land plants tend to contain large-sized mtDNAs, up to 11 Mb in *Silene conica*¹².

mtDNAs of extant species vary markedly in terms of their gene repertoires, genome structure, and genome size, as described above. On top of that, mobile genetic elements confer additional layers of mtDNA diversity.

¹Graduate School of Life and Environmental Sciences, University of Tsukuba, Tsukuba, Japan. ²Center for Computational Sciences, University of Tsukuba, Tsukuba, Japan. ³RIKEN BioResource Research Center, Japan Collection of Microorganisms Microbe Division, Tsukuba, Japan. ⁴Present address: RIKEN BioResource Research Center, Japan Collection of Microorganisms Microbe Division, Tsukuba, Japan. ⁵Present address: Japan Agency for Marine-Earth Science and Technology (JAMSTEC), Yokosuka, Japan. Correspondence and requests for materials should be addressed to Y.N. (email: yuki.nishimura@riken.jp)

Group I introns and group II introns are the examples of the mobile genetic elements found in bacterial, mtDNA and plastid genomes¹³. Group I and group II introns are also known to be able to catalyze self-splicing by forming distinct structures, which enable us to distinguish two types of introns from DNA sequences: Group I introns form the ribozyme structure consisting of 10 stem-loops¹⁴, while group II introns require a characteristic secondary structure, such as a central wheel with six stems, for the self-splicing reaction¹⁵. Both of group I and group II introns show patchy distributions, which are considered to be formed by intron invasion from an intron-containing locus to a homologous, but intron-less locus in the same species and/or a distantly related organisms^{16,17}. Group I intron transfers are facilitated by homing endonucleases (HEs) encoded by introns themselves (Note that HEs can act as maturases that facilitate intron splicing as well¹³). The HEs introduce a double-strand break in the recipient (intron-less) allele that leads to the homologous recombination between intron-containing and intron-less alleles. Individual HEs possess distinct specificities for the nucleotide sequences to recognize and digest. Therefore, a particular HE can introduce the corresponding intron only into a certain position in a genome^{16,18}. Conversely, the group I introns (and the corresponding HEs) found in the homologous position in different genomes are expected to share their evolutionary origin^{19–21}. The mechanism of group II intron transfer is different from that of group I introns, but intron-encoded proteins and their sequence recognition specificities play a central role in invasion for group II intron, as in group I intron. Thus, the evolutionary history of group II introns can be retraced by analyzing intron positions and intron-encoded proteins^{22,23}.

Another type of mobile genetic elements in mitochondria is the linear plasmids²⁴. Typical linear plasmids in mitochondria contain terminal inverted repeats and one or some open reading frames (ORFs) usually encoding virus-type DNA and/or RNA polymerases, designated as *dpo* and *rpo*, respectively, suggesting their independent replication and transcription²⁵. Linear plasmids are extrachromosomal elements in mitochondria, but can occasionally integrate into mtDNA through recombination²⁶. To date, linear plasmids in mitochondria or plasmid-derived *dpo/rpo* sequences in mtDNA have been reported from fungi²⁷, a slime mold²⁸, plants²⁴ and a ciliate²⁹. Consistent with the genetic mobility proposed for the linear plasmids, the phylogenies of *dpo/rpo* were found to be inconsistent with the organismal phylogeny³⁰.

Heliozoa was traditionally defined as a taxonomic group of the axopodium-bearing, heterotrophic unicellular eukaryotes mainly living in freshwater environments³¹. At present, Heliozoa comprises two classes, namely Endohelea and Centrohelea^{32,33}. The phylogenetic position of Heliozoa in the eukaryotes has been controversial for a long time, but recent phylogenomic study suggests that Heliozoa and haptophytes form a monophyletic clade, Haptista, as a sister to the supergroup consisting of stramenopiles, alveolates, and Rhizaria^{34–36}. Although data on the nuclear-encoded genes have been accumulated for heliozoans, as far as we know, no complete mtDNA sequence has been obtained from any member belonging to this group.

Here, we first present the complete mtDNA of a member of the Centrohelea, *Marophrys* sp. strain SRT127. The circular-mapped mtDNA of *Marophrys* contains 69 typical mtDNA-encoded genes. Up to 20 group I introns were found in six out of the 69 genes, and phylogenetic analyses of the corresponding HEs suggested that at least five introns share their origins with those in green algal plastid genomes. We also identified a linear plasmid carrying genes encoding *dpo* and *rpo*. The plasmid is likely to localize in mitochondrion because both mtDNA and plasmid share a deviant genetic code in which UGA codon assigns tryptophan. We further provide the evidence for the linear plasmid being integrated into the mtDNA. These findings expand our knowledge of the diversity of mobile genetic elements in mtDNAs.

Results and Discussion

Mitochondrial genome overview. The mtDNA of a centrohelid *Marophrys* sp. SRT127 is 113,062 bp in length and mapped as circular (Fig. 1). The G + C contents of the mtDNA is 44.7%. It contains 42 kinds of protein-coding genes, which have been vertically inherited from the ancestor of all mitochondria. These 42 protein-coding genes include those for translation elongation factor (*tufA*) and the subunit of cytochrome *c* oxidase assembly (*cox11*), which are notable as most of the mtDNAs do not retain these genes except those in a limited number of eukaryotes^{4,37–42}. In addition, the *Marophrys* mtDNA includes genetically mobile genes, namely those of *dpo*, *rpo* and 11 intronic HEs (see below). The *Marophrys* mtDNA also contains 12 functionally unidentified open reading frames (ORFs) longer than 100 amino acid residues. Large and small subunits of rRNA genes plus 5S rRNA gene were detected. We identified twenty kinds of genes for tRNAs that could translate 50 codons that cover 17 amino acids in total. During our BLAST analyses of the *Marophrys* mtDNA sequence against NCBI nr database, we observed UGA at the conserved tryptophan positions in the putative amino acid sequences. Thus, we concluded that UGA in the *Marophrys* mtDNA is used as tryptophan codon, instead of the termination signal for translation. Genes of the tRNAs that bind the codons UUA for leucine, UGA for tryptophan, ACN for threonine, AAR for lysine and CGN for arginine (R = A or G; N = A, C, G or T) were not found (Table S1). Genes coding for the RNA components for tmRNA and RNAase P could not be detected.

Overview of the introns in the *Marophrys* mtDNA. In the *Marophrys* mtDNA, the genes for cytochrome oxidase *c* subunit 1 (*cox1*), apocytochrome *b* (*cob*), ATP synthetase subunit 1 (*atp1*), and large and small subunits of rRNA (*rnl* and *rns*) appeared to be split by a single or up to nine introns. The sequence motif shared among the canonical group I introns was detected from all of the introns in the *Marophrys* mtDNA (Table 1). A series of RT-PCR experiments confirmed that all of the introns were removed from the mature mRNAs (Fig. S1A). Henceforth here, we designate the introns found in the *Marophrys* mtDNA and those of the HEs harbored in the introns as follows. Introns are designated by adding ‘_i’ (intron) to their host gene names with the ascending numbers from the 5’ terminus (e.g., *rnl_i1* and *rnl_i2* are the first and second introns in the *rnl* gene, respectively). The HEs are distinct from each other by adding the corresponding superscripted host intron names (e.g., HEs harbored in *rnl_i3* and *rnl_i4* are designated as HE^{*rnl_i3*} and HE^{*rnl_i4*}, respectively).

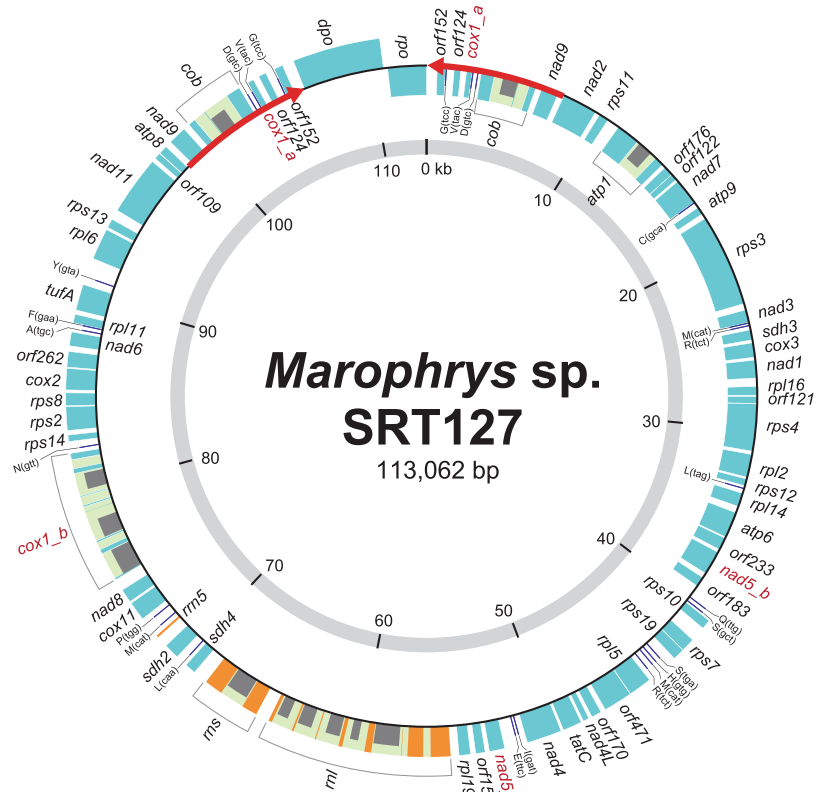


Figure 1. Mitochondrial genome of *Marophrys* sp. SRT127. Protein-coding genes and rRNA genes are shown in the cyan and orange boxes, respectively. Introns are indicated by light green and genes for homing endonuclease (HE) in introns are shown in the gray boxes. The genes for tRNA are depicted as black lines. Two red arrows indicate inverted repeat regions.

The gene for NADH dehydrogenase subunit 5 (*nad5*) appeared to be split into two distant loci in the mtDNA, which were designated as *nad5_a* and *nad5_b* encoding the N- and C-terminal halves of the protein, respectively (Fig. 1). According to the organization of the two loci in the mtDNA, they are most likely transcribed independently. We successfully obtained the evidence for a single, contentious mRNA molecule comprising the transcripts from *nad5_a* and *nad5_b* by performing reverse transcription (RT)-PCR using cDNA as template and two primers—one specific to the *nad5_a* nucleotide sequence and the other to the *nad5_b* nucleotide sequence (Figs 2A and S1B). Thus, the expression of *nad5* most likely requires *trans*-splicing. Likewise, we identified separate loci encoding the N- and C-terminal of Cox1, termed *cox1_a* and *cox1_b*, respectively (Fig. 1). Again, the RT-PCR provided evidence for the transcripts from *cox1_a* and *cox1_b* being *trans*-spliced into a single mRNA molecule encoding the entire Cox1 (Figs 2A and S1B).

RNAweasel suggested that the 3' and 5' flanking region of the transcript from *nad5_a* and *nad5_b* loci, respectively, can form the group I-specific secondary structure together (Fig. 2B–D). Interestingly, two of the predicted stem structures, P7 and P8, can be folded by a combination of the transcripts from *nad5_a* and *nad5_b* loci (Fig. 2C). Therefore, the *trans*-splicing between *nad5_a* and *nad5_b* transcripts is most likely mediated by a group I intron (Fig. 2B–D). Prior to this study, the group I intron-mediated *trans*-splicing was found in the mtDNAs of a placozoan⁴³, green algae^{44,45} and an arbuscular mycorrhizal fungus⁴⁶. However, these examples were limited to the *cox1* and *rnl* genes. Hence, the *Marophrys* mtDNA is the first example of group I intron-mediated *trans*-splicing in *nad5*.

Neither RNAweasel nor Infernal detected any conserved motif of group I (or group II) introns in the nucleotide sequences flanking the *cox1_a* or *cox1_b* locus. Thus, we currently have no insight into the mechanism mediating the *trans*-splicing between the transcripts from the two *cox1* loci.

Origins of group I introns harboring HEs. Overall, 11 of the 19 introns identified in the *Marophrys* mtDNA harbor intronic ORFs encoding LAGLIDADG motif-containing HEs, which have been typically found in group I introns¹⁶. All of the HEs in the *Marophrys* mtDNA belong to either LAGLIDADG_1 (pfam00961) or LAGLIDADG_2 (pfam031611). Here, we explored the evolutionary origins of the 11 group I introns harboring HEs by combining phylogenetic affinities of the HEs and the insertion positions of the introns. We are aware of the cases in which the evolution of a group I intron and that of the corresponding intron-encoded protein disagreed to one another⁴⁷. Unfortunately, we could not examine whether introns and their intron-encoded proteins coevolved, as the intron (nucleotide) sequences dealt in this study are too diverged for phylogenetic

Name	Length (bp)	Intron type ^a	HE type ^b	Shares the ancestry with introns in organellar genomes in green algae? ^c
<i>atp1_i1</i>	1,336	group IB	LAGLIDADG_1	Yes
<i>cob_i1</i>	606	group ID	ND	— ^f
<i>cob_i2</i>	1,351	group IB	LAGLIDADG_2 ^d	No
<i>cox1_i1</i>	1,373	group IB	LAGLIDADG_1 ^d	No
<i>cox1_i2</i>	381	group IB	ND	— ^f
<i>cox1_i3</i>	1,538	group ID	LAGLIDADG_1 ^{d,e}	No
<i>cox1_i4</i>	258	group IB	ND	— ^f
<i>cox1_i5</i>	430	group IB	ND	— ^f
<i>cox1_i6</i>	1,156	group IB	LAGLIDADG_1	No
<i>cox1_i7</i>	462	group IB	ND	— ^f
<i>rnl_i1</i>	381	group IB	ND	— ^f
<i>rnl_i2</i>	297	group IB	ND	— ^f
<i>rnl_i3</i>	1,501	group IA3	LAGLIDADG_1	Yes
<i>rnl_i4</i>	1,137	group IB	LAGLIDADG_2	Yes
<i>rnl_i5</i>	1,177	group IA	LAGLIDADG_2 ^{d,e}	No
<i>rnl_i6</i>	1,138	group IB	LAGLIDADG_2	Yes
<i>rnl_i7</i>	279	group IB	ND	— ^f
<i>rnl_i8</i>	796	group IB2	LAGLIDADG_1	Yes
<i>rns_i1</i>	1,260	group IA	LAGLIDADG_2	Yes

Table 1. Characteristics of introns in the *Marophrys* mtDNA. ^aPredicted by RNAweasel and Infernal. ^bMotifs in intronic ORFs were classified by BLASTP provided by the NCBI website (<https://blast.ncbi.nlm.nih.gov/>). ND - Neither ORF longer than 100 amino acids nor motif was detected. ^cEvolutionary origins of individual introns were inferred by combining phylogenetic analyses of HEs and intron position. ^dHE can be overlapped with upstream exon. ^eHE contains two LAGLIDADG motifs. ^fThe origins of the introns were not assessed, as no intronic ORF was found.

analyses. Thus, we assumed the coevolution of each pair of a group I introns and its HE in the following sections. Table 1 summarizes the group I introns found in the *Marophrys* mtDNA and their putative origins.

Introns sharing the origins with green algal organellar genomes. *Marophrys atp1* intron (*atp1_i1*) harbors an HE (HE^{*atp1_i1*}). The HE phylogeny grouped HE^{*atp1_i1*} with those harbored in *atpA* introns, which were found in the plastid genomes (pDNAs) of green algae belonging to core Chlorophyta, with an ML bootstrap value (MLBP) of 97% (node A in Figs 3 and S2). The *atpA* introns in green algal pDNA and *Marophrys atp1_i1* appeared to be inserted in the homologous positions, namely, phase 0 of the 164th codon for glutamine in *atp1* and the 165th codon for arginine in *atpA* (Figs 3 and S2). The results described above consistently and strongly suggest that lateral transfer of an intron took place between a centrohelid mtDNA and a green algal pDNA. Nevertheless, the data presented above are insufficient to draw definitive conclusions about whether the ancestral intron emerged in an mtDNA or a pDNA. Interestingly, DNA transfer from an mtDNA to a pDNA has been considered to occur rarely^{48,49}, and many cases of DNA transfer with the opposite direction have been documented^{50,51}. Thus, we favor the intron transfer from a green alga to a centrohelid over that in the opposite direction. Moreover, centrohelids probably encounter opportunities to uptake the genetic materials of green algae in the natural environments. *Marophrys* sp. SRT127 and other centrohelids prey on green algae, and some centrohelids are capable of sequestering the plastids of their prey algae for a certain period, which is known as kleptoplasty⁵². Taking these findings together, we propose that *atp1_i1* in the *Marophrys* mtDNA was laterally transferred from a green algal pDNA.

We also detected four *rnl* introns in *Marophrys* mtDNA that shared origins with those in organellar genomes (mtDNAs or pDNAs) in green algae. The HE harbored in *Marophrys rnl_i3* (HE^{*rnl_i3*}) grouped together with the HEs in two mitochondrial and one plastid *rnl* genes in green algae with an MLBP of 97% (node A in Fig. S3). Among the introns harboring the HEs united by node A in Fig. S3, *Marophrys rnl_i3* and two other introns appeared to be inserted in the homologous position (i.e., the introns were found between G¹⁸⁰⁹ and A¹⁸¹⁰; nucleotide numbering is based on the *Marophrys rnl* gene).

The HE harbored in *Marophrys rnl_i4* (HE^{*rnl_i4*}) branched at the base of the clade of nucleus-encoded HEs in land plants with an MLBP of 87% (node A in Fig. S4). The nucleus-encoded HEs in land plants are not encoded by intronic ORFs (designated as “stand-alone” in Fig. S4). *Marophrys* HE^{*rnl_i4*} and the nucleus-encoded HEs were then connected with the HEs harbored in eight plastid and one mitochondrial *rnl* introns in green algae with an MLBP of 85% (node B in Fig. S4). In the clade united by node B, HE^{*rnl_i4*} was excluded from both stand-alone HEs in land plants, and HEs in organellar *rnl* introns in green algae. It is difficult to clarify the origin of HE^{*rnl_i4*} with a confidence based on the HE phylogeny (Fig. S4). However, the particular HE in the *Marophrys* mtDNA is encoded by an intronic ORF (not by a stand-alone), and *Marophrys rnl_i4* and eight plastid *rnl* introns in green algae appeared to be inserted between T²¹⁵¹ and C²¹⁵² (nucleotide numbering is based on the *Marophrys rnl* gene). Taking these findings together, we propose that *Marophrys rnl_i4* and the eight *rnl* introns in green algal pDNA are derived from a single *rnl* intron.

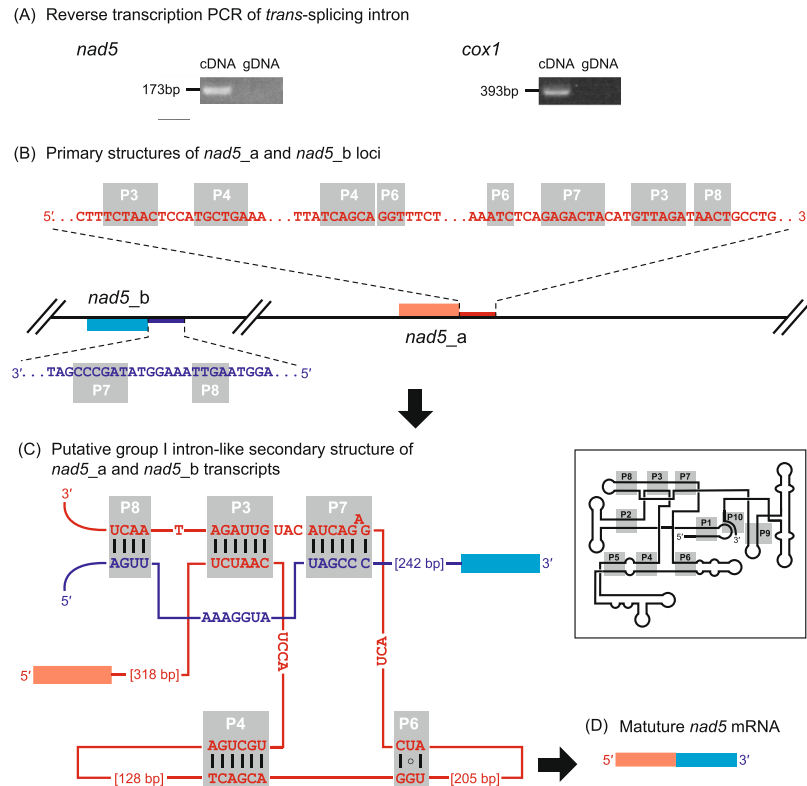


Figure 2. *Trans*-splicing for *nad5* and *cox1* gene expressions in the *Marophrys* mitochondrial genome. (A) Reverse transcription PCR using a set of primers specific to *nad5_a* and *nad5_b* loci (left) and that specific to *cox1_a* and *cox1_b* loci (right). The DNA fragment was amplified from the cDNA template which most likely contained the spliced product connecting the two RNA fragments transcribed from the two separate loci together (lanes labelled with “cDNA”). On the other hand, no specific amplification was observed in the PCR using the genomic DNA template due to the configuration of the two separate loci in the mtDNA (lanes labelled with “gDNA”). (B–C) Model for *nad5* mRNA *trans*-splicing. (B) Primary structures of *nad5_a* and *nad5_b* loci. mtDNA, exons, and introns are shown in thin black lines, boxed, and thick lines, respectively. The 5' exon and subsequent intronic region are colored in red, while the 3' exon and its preceding intronic region are indicated in blue. The two loci are located on the different strands, and thus transcribed independently from each other. (C) Putative group I intron-like secondary structure of *nad5_a* and *nad5_b* transcripts. Five stem-loop structures conserved among group I intron ribozymes (P3, P4, P6, P7, and P8) can be formed within the *nad5_a* transcript and between the *nad5_a* and *nad5_b* transcripts. This secondary structure was predicted by RNAweasel followed by manual inspection and modification. Watson–Crick base pairings and a wobble bond in the five stem-loop structures are indicated by the black lines and a circle, respectively. The typical secondary structure of group I intron ribozymes is schematically shown as an inset. (D) Mature *nad5* mRNA.

The HE harbored in *Marophrys rnl_i6* (HE^{rnl_i6}) and those found in four plastid and four mitochondrial *rnl* introns in green algae formed a clade with an MLBP of 91% (node C in Fig. S4). Among the introns harboring the HEs united by node C in Fig. S4, the *Marophrys* intron was found to share the insertion position with three plastid introns (i.e., the introns were found between C²³⁹⁴ and A²³⁹⁵; nucleotide numbering is based on the *Marophrys rnl* gene). We concluded that *Marophrys rnl_i6* and the *rnl* introns found in green algal organellar genomes share the common ancestor.

The HE harbored in *Marophrys rnl_i8* (HE^{rnl_i8}) and that in the *rnl* intron in the *Acanthamoeba castellanii* mtDNA grouped together with an MLBP of 94%, and the two introns appeared to be inserted between G²⁴⁸² and A²⁴⁸³ (nucleotide numbering is based on the *Marophrys rnl* gene; node A in Fig. S5). Moreover, the clade of HE^{rnl_i8} and the *Acanthamoeba* HE clustered with two stand-alone HEs in bacterial genomes, HEs found in 24 *rnl* introns in green algal mtDNAs/plDNAs and a single *rnl* intron in a diatom mtDNA (MLBP = 86%, node B in Fig. S5). The vast majority of the *rnl* introns described here were found in a homologous position. Altogether, we suspect that the ancestral intron, which gave rise to the ones in the *Marophrys* and *Acanthamoeba* mt *rnl* genes, resided in the *rnl* gene in a green algal mtDNA or plDNA.

By combining the phylogenetic affinities of HEs and intron positions, we propose that the four *rnl* HEs (and their host introns) found in the *Marophrys* mtDNA share origins with those in organellar genomes in green algae as well as those of *atp1*. The *atp1* and *rnl* introns described above were likely transmitted from green algae to *Marophrys* by considering the predator–prey relationship between centrohelids and green algae in the wild (see above). We presume that, once mobile genetic elements resided in a centrohelid mtDNA, these elements

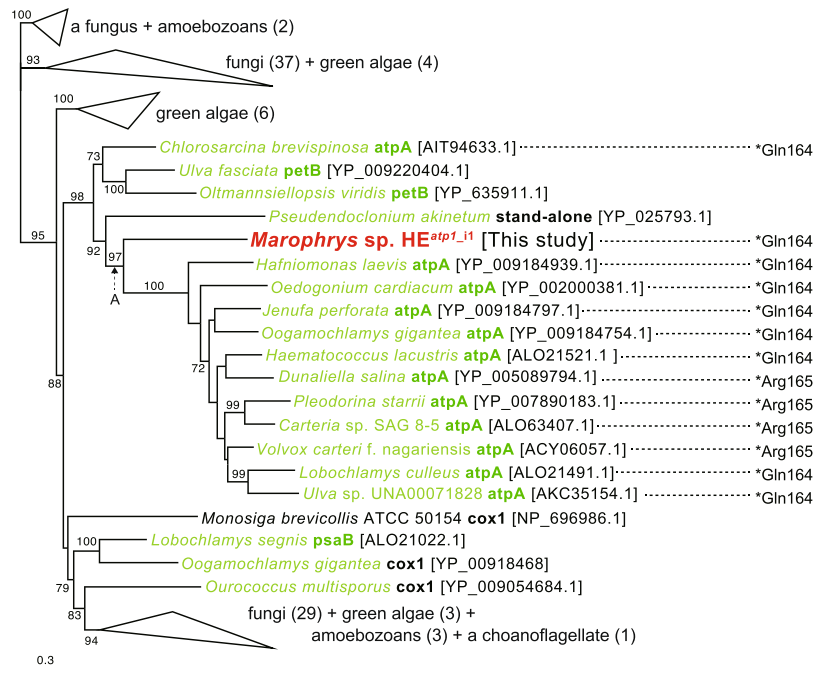


Figure 3. Maximum likelihood (ML) analysis of the homing endonucleases harbored in the first intron in *atp1* (HE^{atp1_i1}) in the *Marophrys* mitochondrial genome. OTU names consist of species name, intron-hosting gene (bold) and accession number in brackets. Green algal sequences are shown in green. Gene names are colored in green when they reside in plastid genomes. The inserted positions of *atpA/atp1* introns are presented the numbers of the amino acid residues correspond to the *Marophrys* sequence. Asterisks indicate insertion site in triplet codon. For instance, “*Gln164” means that an intron was found between the codon for Gln¹⁶⁴ and that for the 163th amino acid (phase class = 0). Ultrafast bootstrap values higher than 70% are shown. Collapsed clades are indicated by triangles and the lineages included in the clade are shown with the number of genes in parentheses. The detailed ML tree is given in Fig. S2.

may have persisted in the descendant genomes, as centrohelids are unicellular and asexual eukaryotic lineage⁵³. Unfortunately, the data obtained in this study failed to (i) pinpoint the green algal species that donated the five introns or (ii) clarify whether mtDNA or plDNA was the origin of each of the four *rnl* introns. It is also important to re-examine the putative green algal origins of the five introns (and their HEs) in future studies incorporating organellar genome data sampled from much broader eukaryotes (green algae and centrohelids in particular).

It should be noted that, in the strict sense, we cannot rule out the possibility of intron-HE coevolution being violated in the *Marophrys* mtDNA, as the intron phylogenies were not examined due to their extremely divergent natures. Nevertheless, the HE phylogenies (Figs 3 and S2–5) firmly suggest that the HE-coding DNA fragments were transferred from green algal organellar genomes to centrohelid mtDNAs.

Other introns. The HE found in *Marophrys rns_i1* was placed within a radiation of the HEs in *rns* genes in green algal plastid and bacterial genomes, and this clade received an MLBP of 96% (node D in Fig. S4). Within this clade, the affinity between the *Marophrys* and bacterial HEs could not be excluded, leaving the origin of this intron inconclusive.

The HE phylogeny tied together the HE found in *Marophrys cob_i2* and that in a fungal *cob* intron with an MLBP of 86% (node E in Fig. S4). However, the inserted positions of the two *cob* introns appeared to be distant from each other. Thus, it remains unclear whether the two *cob* introns genuinely share the same origin.

The HE phylogeny united the HE found in *Marophrys cox1_i1* (HE^{cox1_i1}) and those in two green algal and three fungal *cox1* genes with an MLBP of 78% (node A in Fig. S6). However, HE^{cox1_i1} showed no special affinity to any of the five HEs in this clade. The inserted positions of *Marophrys cox1_i1* and those harboring the five HEs grouped with HE^{cox1_i1} appeared to vary. We consider that the results described above are insufficient to infer the origin of *Marophrys cox1_i1* with confidence.

As we yielded no insight for the origin of *cox1_i3*, *cox1_i6* or *rnl_i5*, as none of their HEs showed any particular affinities to other HEs considered in the analyses (Figs S4 and S7).

Plasmid and plasmid-derived genes. In addition to the circular mtDNA, we identified a linear plasmid of 5,877 bp in length with inverted repeats at both ends (Fig. S8). This plasmid contains genes encoding virus-type *dpo* and *rpo* (Fig. S8). The two genes in the *Marophrys* plasmid most likely use UGA for tryptophan codon instead of translation termination signal. Although no experimental evidence is available, we consider that the linear plasmid localizes in the *Marophrys* mitochondrion for two reasons described below. First, the structure and gene

content of the *Marophrys* plasmid resemble those of mitochondrial plasmids found in land plants, fungi, amoeba and a ciliate *Oxytricha trifallax*^{24–29}. Second, the circular mtDNA and linear plasmid share the same deviant genetic code. Given the patchy distribution in the tree of eukaryote, the linear plasmids are regarded as one of the mobile genetic elements^{23,29,54}. Altogether, we here propose that the *Marophrys* plasmid was laterally acquired from an as-yet-unknown eukaryote.

The *Marophrys* plasmid showed clear similarity at the nucleotide level to the region containing *dpo* and *rpo* in the circular mtDNA (Fig. S8). As observed in other eukaryotes^{25,54}, we suspect that the linear plasmid was integrated into the circular mtDNA in the *Marophrys* mitochondrion⁵⁵. The inverted repeats were proposed to facilitate the linear plasmid to integrate into an mtDNA, and, in some cases, the entire plasmid including the repeats were found in the mtDNA⁵⁶. In the *Marophrys* mitochondrion, the inverted repeats in the linear plasmid (102 bp in length) were found to be totally different from those surrounding *dpo* and *rpo* in the mtDNA (the regions highlighted by red arrows in Fig. 1; 7,659 bp), indicating that only two genes in the plasmid were integrated into the mtDNA. Nevertheless, it is attractive to hypothesize that plasmid integration (more precisely integration of *dpo* and *rpo*) triggered the duplication of a ~7.6 Kb region containing *nad9*, *cob*, *cox1_a*, two ORF and three tRNA genes observed in the current *Marophrys* mtDNA (red arrows in Fig. 1), as Sakurai *et al.*⁵⁷ reported the structural change in an mtDNA led by plasmid integration. Unfortunately, the mtDNA from a single centrohelid species is insufficient to examine whether the inverted repeats in the *Marophrys* mtDNA arose with the plasmid integration. Relevant to the above issue, we need to clarify the mechanism by which plasmid integration introduced the inverted repeats in the recipient DNA molecule. As the first step toward resolving the issues mentioned above, we require additional mtDNA data from multiple centrohelids, particularly close relatives of *Marophrys*.

Methods

Isolation and culturing. A clonal culture of a centrohelid (strain SRT127) was established using micropipetting method from seawater sample that had been collected from Tokyo Bay, Tokyo, Japan (35.6281°N, 139.7713°E), on July 30, 2011. Based on the morphological characteristics, strain SRT127 was identified as a member of the genus *Marophrys* (Fig. S9).

Marophrys sp. strain SRT127 was maintained in MNK medium (<http://mcc.nies.go.jp/02medium.html#mnk>) with a green alga *Pyramimonas* sp. as prey at 20 °C under a 14-h light / 10-h dark cycle until it died in March 2016.

DNA/RNA extraction and cDNA synthesis. The centrohelid cells were collected by centrifugation once they had reached confluence and the algal cells were hardly observed in the culture medium under a light microscope. Genomic DNA was extracted with 25:24:1 of phenol:chloroform:isoamyl alcohol and purified by ethanol precipitation. Total RNA was extracted using TRIzol (Thermo Fisher Scientific), following manufacturer's instructions. The extracted RNA was used to synthesize random hexamer-primed cDNA with SuperScript II reverse transcriptase (Thermo Fisher Scientific). The cDNA was used for the PCR experiments to confirm intron splicing (see detail in *Genome annotation* section).

Sequencing of the *Marophrys* sp. mitochondrial genome. Approximately 10 µg of the extracted DNA was submitted to Illumina Sequencing technology (HiSeq 2000 at Eurofins Genomics). A total of 125,733,479 paired-end reads of 100 bp were generated (Approx. 25 Gb in total) and assembled by SPAdes⁵⁸. To identify mitochondrial sequences from the assembly data, a TBLASTN⁵⁹ search was performed using the putative amino acid sequences of mitochondrion-encoded proteins in a jakobid *Andalucia godoyi*⁴ as queries. A total of 228 contigs were recovered as candidates for *Marophrys* mtDNA fragments at the threshold *E*-value of < 1e−10. Then, the candidate contigs were used as a queries for a BLASTN⁵⁹ search against the NCBI non-redundant nucleotides database. The contigs hit to bacterial sequences with ≥ 95% nucleotide identity in the second BLAST analysis were discarded as the genome fragments originated from bacteria contaminating in the *Marophrys* culture. After filtering bacterial sequences, two contigs, which were 90,947 and 7,652 bp in length, were recovered as mtDNA fragments of *Marophrys*. By mapping the paired-end reads on the two putative mtDNA fragments using Bowtie2⁶⁰, we additionally identified a contig of 6,811 bp in length as a mtDNA fragment. The third contig was overlooked by the first TBLASTN⁵⁹ analysis, as this region only carries *dpo* and *rpo* genes that encode non-typical mitochondrion-encoded proteins. The physical continuity of three candidate mtDNA fragments was confirmed by PCR. Finally, the *Marophrys* mtDNA was reconstructed as a circular molecule of 113,062 bp in length.

Linear plasmid carrying *dpo* and *rpo*. A contig of 5,877 bp in length was found by a TBLASTN⁵⁹ search against the assembly data using the *dpo* and *rpo* genes identified in the circular-mapped mtDNA as queries. This 5,877 bp-contig appeared to bear inverted repeats of 102 bp in length at both 5' and 3' ends, and to carry only *dpo* and *rpo*. To determine whether the contig is a linear or circular molecule, we mapped the paired-end reads to the contig using Bowtie2⁶⁰. We also conducted a PCR experiment to connect both ends of the contig as done to the circular mtDNA (see above). As neither of the aforementioned experiments positively supported the circular structure of the contig (data not shown), we concluded that the 5,877-bp contig represents a linear DNA molecule.

Genome annotation. The *Marophrys* mtDNA was annotated by Prokka⁶¹, followed by manual curation. NCBI translational Table 4 (<https://www.ncbi.nlm.nih.gov/Taxonomy/Utils/wprintgc.cgi#SG4>) was applied during the aforementioned annotation, because UGA codons are most likely assigned as tryptophan, not as the termination signal for translation in the *Marophrys* mtDNA. When a gene appeared to contain one or more introns, the corresponding cDNA was amplified by PCR with the primers listed in Table S2, and the amplicons (Fig. S1A,B) were sequenced by the Sanger method. The precise intron–exon boundaries were determined by comparing the corresponding cDNA and genome sequences. The type of introns was predicted by RNAweasel (<http://megasun.bch.umontreal.ca/cgi-bin/RNAweasel/RNAweaselInterface.pl>). The secondary structural motif conserved among group I introns was also searched by Infernal⁶² with covariance models built by Nawrocki *et al.*⁶³.

Phylogenetic analyses of HEs. The conceptual amino acid sequences of the HEs identified in the *Marophrys* mtDNA were used as queries for a BLASTP⁵⁹ search against the NCBI nr database (*E*-values threshold < 1e−10) to generate phylogenetic datasets of HEs. The HE sequences retrieved from the NCBI nr database, which shared >90% identity at the amino acid sequence level, were clustered by CD-HIT^{64,65}. To reduce the redundancy, the representative sequences from each cluster were selected to build the phylogenetic datasets analyzed in this study. The HE sequences harbored in the third and sixth introns of *cox1* gene appeared to share the same evolutionary origin, and we prepared a single dataset including both HEs and their related sequences. For a similar reason, we prepared a single dataset containing HEs harbored in three of the introns found in *rnl* gene, a single intron in *rns* gene and one of the introns found in *cob* gene in the *Marophrys* mtDNA. Individual datasets were subjected to MAFFT⁶⁶ with the LINSI option for calculating the alignments. The ambiguously aligned sites in the alignments were discarded manually. Maximum likelihood (ML) analyses using IQ-TREE⁶⁷ were conducted on each alignment with 1,000 ultrafast bootstrap replicates⁶⁸. The substitution models were selected by ModelFinder⁶⁹ implemented in IQ-TREE.

Data Availability

The *Marophrys* mtDNA sequences with annotation are available at GenBank/EMBL/DDBJ (accession nos AP019310 and AP019311). The alignments of HEs used to estimate phylogenetic tree are available from the corresponding author on request.

References

- Karnkowska, A. *et al.* A Eukaryote without a mitochondrial organelle. *Curr. Biol.* **26**, 1274–84 (2016).
- Treitli, S. C. *et al.* Molecular and Morphological Diversity of the Oxymonad Genera *Monocercomonoides* and *Blattamonas* gen. nov. *Protist* **169**(5), 744–783 (2018).
- Gray, M. W., Lang, B. F. & Burger, G. Mitochondria of protists. *Annu. Rev. Genet.* **38**, 477–524 (2004).
- Burger, G., Gray, M. W., Forget, L. & Lang, B. F. Strikingly bacteria-like and gene-rich mitochondrial genomes throughout jakobid protists. *Genome Biol. Evol.* **5**, 418–38 (2013).
- Roger, A. J., Muñoz-Gómez, S. A. & Kamikawa, R. The origin and diversification of mitochondria. *Curr. Biol.* **27**, R1177–92 (2017).
- Flegentov, P. *et al.* Divergent mitochondrial respiratory chains in phototrophic relatives of apicomplexan parasites. *Mol. Biol. Evol.* **32**, 115–31 (2015).
- Vahrenholz, C., Riemen, G., Pratje, E., Dujon, B. & Michaelis, G. Mitochondrial DNA of *Chlamydomonas reinhardtii*: the structure of the ends of the linear 15.8-kb genome suggests mechanisms for DNA replication. *Curr. Genet.* **24**, 241–7 (1993).
- Hikosaka, K., Kita, K. & Tanabe, K. Diversity of mitochondrial genome structure in the phylum Apicomplexa. *Mol. Biochem. Parasitol.* **188**, 26–33 (2013).
- Nishimura, Y. *et al.* Mitochondrial genome of *Palpitomonas bilixi*: Derived genome structure and ancestral system for cytochrome *c* maturation. *Genome Biol. Evol.* **8**(3090–98), 2016 (2016).
- Burger, G., Forget, L., Zhu, Y., Gray, M. Q. & Lang, F. Unique mitochondrial genome architecture in unicellular relatives of animals. *Proc. Natl. Acad. Sci. USA* **100**, 892–7 (2003).
- Smith, D. R. *et al.* First complete mitochondrial genome sequence from a box jellyfish reveals a highly fragmented linear architecture and insights into telomere evolution. *Genome Biol. Evol.* **4**, 52–8 (2012).
- Sloan, D. B. *et al.* Rapid evolution of enormous, multichromosomal genomes in flowering plant mitochondria with exceptionally high mutation rates. *PLoS Biol.* **10**, e1001241, <https://doi.org/10.1371/journal.pbio.1001241> (2012).
- Lang, B. F., Laforest, M. J. & Burger, G. Mitochondrial introns: a critical view. *Trends Genet.* **23**, 119–25 (2007).
- Hausner, G., Hafez, M. & Edgell, R. Bacterial group I introns: mobile RNA catalysts. *Mob. DNA* **5**, 8, <https://doi.org/10.1186/1759-8753-5-8>. (2014).
- Toro, N. Bacterial and Archaea group II introns: additional mobile genetic elements in the environment. *Environ. Microbiol.* **5**, 143–51 (2003).
- Haugen, P., Simon, D. M. & Bhattacharya, D. The natural history of group I introns. *Trends Genet.* **21**, 111–9 (2005).
- Zimmerly, S. & Semper, C. Evolution of group II introns. *Mob. DNA* **6**, 7, <https://doi.org/10.1186/s13100-015-0037-5> (2014).
- Belfort, M. & Roberts, R. J. Homing endonucleases: keeping the house in order. *Nucleic Acids Res.* **25**, 3379–88 (1997).
- Cho, Y., Qiu, Y. L., Kuhlman, P. & Palmer, J. D. Explosive invasion of plant mitochondria by a group I intron. *Proc. Natl. Acad. Sci. USA* **95**, 14244–9 (1998).
- Sanchez-Puerta, M. V. *et al.* phylogenetic local horizontal transfer of the *cox1* group I intron in flowering plant mitochondria. *Mol. Biol. Evol.* **25**, 1762–77 (2008).
- Nishimura, Y., Kamikawa, R., Hashimoto, T. & Inagaki, Y. Separate origins of group I intron in two mitochondrial genes of the katablepharid *Leucocryptos marina*. *PLoS One* **7**, e37307, <https://doi.org/10.1371/journal.pone.0037307> (2012).
- Bonen, L. & Vogel, J. The ins and outs of group II introns. *Trends Genet.* **17**, 322–31 (2001).
- Toor, N., Hausner, G. & Zimmerly, S. Coevolution of group II intron RNA structures with their intron-encoded reverse transcriptases. *RNA* **7**, 1142–52 (2001).
- Handa, H. Linear plasmid in plant mitochondria: peaceful coexistences or malicious invasions? *Mitochondrion* **8**, 15–25 (2008).
- Kuzmin, E. V. & Levchenko, I. V. S1 plasmid from cms-S-maize mitochondria encodes a viral type DNA-polymerase. *Nucleic Acids Res.* **15**, 6758 (1987).
- Bertrand, H., Griffiths, A. J., Court, D. A. & Cheng, C. K. An extrachromosomal plasmid is the etiological precursor of *kal*DNA insertion sequences in the mitochondrial chromosome of senescent *Neurospora*. *Cell* **47**, 829–37 (1986).
- Chan, B. S., Court, D. A., Vierula, P. J. & Bertrand, H. The *kal* linear senescence-inducing plasmid of *Neurospora* is an invertron and encodes DNA and RNA polymerases. *Curr. Genet.* **20**, 225–37 (1991).
- Takano, H., Kawano, S. & Kuroiwa, T. Genetic organization of a linear mitochondrial plasmid (mF) that promotes mitochondrial fusion in *Physarum polycephalum*. *Curr. Genet.* **26**, 506–11 (1994).
- Swart, E. C. *et al.* The *Oxytricha trifallax* mitochondrial genome. *Genome Biol. Evol.* **4**, 136–54 (2012).
- Warren, J. M., Simmons, M. K., Wu, Z. & Sloan, D. B. Linear plasmids and the rate of sequence evolution in plant mitochondrial genomes. *Genome Biol. Evol.* **8**, 364–74 (2016).
- Mikrjukov, K. A. System and phylogeny of Heliozoa: should this taxon exist in modern systems in protists? *Zool Z.* **79**, 883–97 (2000).
- Yabuki, A., Chao, E. E., Ishida, K. & Cavalier-Smith, T. *Microheliella maris* (Microhelida ord. n.), an ultrastructurally highly distinctive new axopodial protist species and genus, and the unity of phylum Heliozoa. *Protist* **163**, 356–88 (2012).
- Cavalier-Smith, T., Chao, E. E. & Lewis, R. Multiple origins of Heliozoa from flagellate ancestors: New cryptist subphylum Corbihelia, superclass Corbistoma, and monophyly of Haptista, Cryptista, Hacrobia and Chromista. *Mol. Phylogenet. Evol.* **93**, 331–62 (2015).

34. Sakaguchi, M., Nakayama, T., Hashimoto, T. & Inouye, I. Phylogeny of the Centrohelida inferred from SSU rRNA, tubulins, and actin genes. *J. Mol. Evol.* **61**, 765–75 (2005).
35. Burki, F., Okamoto, N., Pombert, J. F. & Keeling, P. J. The evolutionary history of haptophytes and cryptophytes: phylogenomic evidence for separate origins. *Proc. Biol. Sci.* **279**, 2246–54 (2012).
36. Burki, F. *et al.* Untangling the early diversification of eukaryotes: a phylogenomic study of the evolutionary origins of Centrohelida, Haptophyta and Cryptista. *Proc. Biol. Sci.* **283**, 20152802, <https://doi.org/10.1098/rspb.2015.2802> (2016).
37. Lang, B. F. *et al.* An ancestral mitochondrial DNA resembling a eubacterial genome in miniature. *Nature* **387**, 493–7 (1997).
38. Herman, E. K. *et al.* The mitochondrial genome and a 60-kb nuclear DNA segment from *Naegleria fowleri*, the causative agent of primary amoebic meningoencephalitis. *J. Eukaryot. Microbiol.* **60**, 179–91 (2013).
39. Fučíková, K. & Lahr, D. J. Uncovering cryptic diversity in two Amoebozoan species using complete mitochondrial genome sequences. *J. Eukaryot. Microbiol.* **63**, 112–22 (2016).
40. Kamikawa, R., Shiratori, T., Ishida, K., Miyashita, H. & Roger, A. J. Group II intron-mediated *trans*-splicing in gene-rich mitochondrial genome of an enigmatic eukaryote. *Diphylleia rotans*. *Genome Biol. Evol.* **3**, 458–66 (2016).
41. Janouškovec, J. *et al.* A new lineage of eukaryotes illuminates early mitochondrial genome reduction. *Curr. Biol.* **27**, 3717–24 (2017).
42. Yabuki, A., Gyaltsen, Y., Heiss, A. A., Fujikura, K. & Kim, E. Ophirina amphinema n. gen., n. sp., a New Deeply Branching Discobid with Phylogenetic Affinity to Jakobids. *Scientific Reports* **8**(1) (2018).
43. Burger, G., Yan, Y., Javadi, P. & Lang, B. F. Group I-intron *trans*-splicing and mRNA editing in the mitochondria of placozoan animals. *Trends Genet.* **25**, 381–6 (2009).
44. Pombert, J. F. & Keeling, P. J. The mitochondrial genome of the entomoparasitic green alga *Helicosporidium*. *PLoS One* **5**, e8954, <https://doi.org/10.1371/journal.pone.0008954> (2010).
45. Pombert, J. F., Otis, C., Turmel, M. & Lemieux, C. The mitochondrial genome of the prasinophyte *Prasinoderma coloniale* reveals two *trans*-spliced group I introns in the large subunit rRNA gene. *PLoS One* **8**, e84325, <https://doi.org/10.1371/journal.pone.0084325> (2013).
46. Nadimi, M., Beaudet, D., Forget, L., Hijri, M. & Lang, B. Group I intron-mediated *trans*-splicing in mitochondria of *Gigaspora rosea* and a robust phylogenetic affiliation of arbuscular mycorrhizal fungi with Mortierellales. *Mol. Biol. Evol.* **29**, 2199–210 (2012).
47. Haugen, P. *et al.* The recent transfer of a homing endonuclease gene. *Nucleic Acids Res.* **33**, 2734–41 (2005).
48. Bock, R. The give-and-take of DNA: horizontal gene transfer in plants. *Trends Plant Sci.* **15**, 11–22 (2010).
49. Iorizzo, M. *et al.* *De novo* assembly of the carrot mitochondrial genome using next generation sequencing of whole genomic DNA provides first evidence of DNA transfer into an angiosperm plastid genome. *BMC Plant Biol.* **12**, 61, <https://doi.org/10.1186/1471-2229-12-61> (2012).
50. Turmel, M. *et al.* Evolutionary transfer of ORF-containing group I introns between different subcellular compartments (chloroplast and mitochondrion). *Mol. Biol. Evol.* **12**, 533–45 (1995).
51. Alverson, A. J. *et al.* Insights into the evolution of mitochondrial genome size from complete sequences of *Citrullus lanatus* and *Cucurbita pepo* (Cucurbitaceae). *Mol. Biol. Evol.* **27**, 1436–48 (2010).
52. Patterson, D. J. & Dürschmidt, M. Selective retention of chloroplasts by algivorous heliozoa: Fortuitous chloroplast symbiosis? *Eur. J. Protistol.* **23**, 51–5 (1987).
53. Speijer, D., Lukeš, J. & Eliáš, M. Sex is a ubiquitous, ancient, and inherent attribute of eukaryotic life. *Proc. Natl. Acad. Sci. USA* **112**, 8827–34 (2015).
54. Robison, M. M. & Wolyn, D. J. A mitochondrial plasmid and plasmid-like RNA and DNA polymerases encoded within the mitochondrial genome of carrot (*Daucus carota* L.). *Curr. Genet.* **47**, 57–66 (2005).
55. Court, D. A. & Bertrand, H. Genetic organization and structural features of *maranhar*, a senescence-inducing linear mitochondrial plasmid of *Neurospora crassa*. *Curr. Genet.* **22**, 385–97 (1992).
56. Sakurai, R., Sasaki, N., Takano, H., Abe, T. & Kawano, S. *In vivo* conformation of mitochondrial DNA revealed by pulsed-field gel electrophoresis in the true slime mold, *Physarum polycephalum*. *DNA Res.* **7**, 83–91 (2000).
57. Hausner, G. Introns, mobile elements and plasmids. In *Organelle Genetics: Evolution of Organelle Genomes and Gene Expression*. (Ed. Bullerwell, C. E.) 329–358 (Springer Verlag, 2012).
58. Nurk, S. *et al.* Assembling single-cell genomes and mini-metagenomes from chimeric MDA products. *J. Comput. Biol.* **20**, 714–37 (2013).
59. Altschul, S. F., Gish, W., Miller, W., Myers, E. W. & Lipman, D. J. Basic local alignment search tool. *J. Mol. Biol.* **215**, 403–10 (1990).
60. Langmead, B. & Salzberg, S. L. Fast gapped-read alignment with Bowtie 2. *Nat. Methods.* **9**, 357–9 (2012).
61. Seemann, T. Prokka: rapid prokaryotic genome annotation. *Bioinformatics* **30**, 2068–9 (2014).
62. Nawrocki, E. P. & Eddy, S. R. Infernal 1.1: 100-fold faster RNA homology searches. *Bioinformatics* **29**, 2933–35 (2013).
63. Nawrocki, E. P., Jones, T. A. & Eddy, S. R. Group I introns are widespread in archaea. *Nucleic Acids Res.* **46**, 7970–76 (2018).
64. Li, W. & Godzik, A. Cd-hit: a fast program for clustering and comparing large sets of protein or nucleotide sequences. *Bioinformatics* **22**, 1658–9 (2006).
65. Fu, L., Niu, B., Zhu, Z., Wu, S. & Li, W. CD-HIT: accelerated for clustering the next-generation sequencing data. *Bioinformatics* **28**, 3150–2 (2012).
66. Katoh, K., Kuma, K., Toh, H. & Miyata, T. MAFFT version 5: improvement in accuracy of multiple sequence alignment. *Nucleic Acids Res.* **33**, 511–8 (2005).
67. Nguyen, L. T., Schmidt, H. A., von Haeseler, A. & Minh, B. Q. IQ-TREE: A fast and effective stochastic algorithm for estimating maximum-likelihood phylogenies. *Mol. Biol. Evol.* **32**, 268–74 (2015).
68. Hoang, H. C., Chernomor, O., von Haeseler, A., Minh, B. Q. & Vinh, L. S. UFBBoot2: Improving the ultrafast bootstrap approximation. *Mol. Biol. Evol.* **35**, 518–22 (2018).
69. Kalyaanamoorthy, S., Minh, B. Q., Wong, T. K. F., von Haeseler, A. & Jeremiin, L. S. ModelFinder: Fast model selection for accurate phylogenetic estimates. *Nat. Methods.* **14**, 587–9 (2017).

Acknowledgements

This work was supported in part by grants from the Japanese Society for Promotion of Science awarded to Y.N. (18K14783), Y.I. (23117006, 16H04826 and 18KK0203) and T.H. (23117005 and 15H05231). This work was also supported, in part by the RIKEN Competitive Program for Creative Science and Technology (to M.O.). Y. N. was supported by a Research Fellowships from the JSPS for Young Scientists (no. 25789).

Author Contributions

Y.N. conceived and designed experiments. Y.N. and T.S. performed experiments. Y.N. and Y.I. analyzed the data. Y.N., T.S., K.I., T.H., M.O., and Y.I. discussed results and implications. Y.N. and Y.I. wrote the manuscript and all authors joined in revision. T.H. and Y.I. supervised Y.N. K.I. supervised T.S.

Additional Information

Supplementary information accompanies this paper at <https://doi.org/10.1038/s41598-019-41238-6>.

Competing Interests: The authors declare no competing interests.

Publisher's note: Springer Nature remains neutral with regard to jurisdictional claims in published maps and institutional affiliations.



Open Access This article is licensed under a Creative Commons Attribution 4.0 International License, which permits use, sharing, adaptation, distribution and reproduction in any medium or format, as long as you give appropriate credit to the original author(s) and the source, provide a link to the Creative Commons license, and indicate if changes were made. The images or other third party material in this article are included in the article's Creative Commons license, unless indicated otherwise in a credit line to the material. If material is not included in the article's Creative Commons license and your intended use is not permitted by statutory regulation or exceeds the permitted use, you will need to obtain permission directly from the copyright holder. To view a copy of this license, visit <http://creativecommons.org/licenses/by/4.0/>.

© The Author(s) 2019